LINKING LARGE-SCALE WET-SNOW SPATIAL PATTERNS IN MOUNTAINOUS TERRAIN TO INCIDENT RADIATION AND TOPOGRAPHY

N. Helbig*, F. Techel, A. van Herwijnen and T. Jonas

WSL Institute for Snow and Avalanche Research SLF, Davos, Switzerland

ABSTRACT: Water percolating through the snow cover can lead to wet-snow instability as well as snowmelt runoff. The accurate prediction of spatial patterns of wet-snow in mountainous terrain therefore has practical applications in both hydrological and avalanche forecasting. Recent research has shown that incident radiation plays a dominant role during the first wetting of the snow cover. We therefore investigated if large-scale meteorological forecast data, corrected for subgrid topographic influences on the shortwave radiation balance, together with subgrid mean slopes can be combined to improve the prediction of large-scale wet-snow avalanche patterns. Required surface albedo was derived from parameterized snow covered fraction based on terrain parameters and measured flat field snow depths. We derived avalanche probability density functions (pdf) for daily mean air temperature and incoming short wave radiation from detailed observations over six winters using time-lapse photography. Based on these pdf's, we computed wet-snow probability maps for a scale of a few kilometers. The probability maps compared well with observed wet-snow avalanche activity patterns. Even though, our method clearly needs to be extended to include snow cover related parameters, it provides a new approach towards an automatic avalanche forecast built upon simple terrain parameters and easy to obtain large-scale meteorological surface variables. The advantage of our method is that it does not require running any sophisticated, small-scale models with demanding model input parameters.

KEYWORDS: wet-snow; avalanche forecasting; meteorological models; subgrid parameterization.

1. INTRODUCTION

Operational avalanche forecasting mainly relies on meteorological observations and forecasts in combination with snow cover instability observations, ideally direct observations of avalanches (e.g. McClung and Schaerer (2006)). It involves the assimilation of multiple data sources to make predictions over complex interacting processes. To date, the employed methods are largely based on experience of the forecaster and are prone to subjectiveness and difficult to transfer to new personnel. Numerous attempts have been made to develop objective avalanche forecasting techniques. Such efforts predominantly consist of statistically relating local weather observations with avalanche occurrence data or estimated danger (e.g. Buser (1983); Pozdnoukhov et al. (2011); Schweizer and Föhn (1996)). Statistical forecasting models are based on the idea that similar weather conditions lead to comparable avalanche situations. Depending on the scale of the study area and the quality of the input data, the accuracy of the statistical models can vary greatly. A major drawback is the poor temporal and spatial resolution of avalanche observations to validate the models.

Recently new tools were developed to forecast wet-snow avalanches (Mitterer et al. (2013a)), since a common method where air temperature is related to wet-snow instabilities (Kattelmann (1985)) was shown to produce too many false alarms (Mitterer and Schweizer (2012); Trautman (2008)). By introducing a combination of air and snow surface temperature, or by modeling the entire energy balance for virtual slopes, avalanche and non-avalanche days were classified with reasonable accuracy (Mitterer et al. (2013b)). However, modeling the energy balance at a scale relevant for regional avalanche forecasting is computationally very costly and is not yet done operationally. Nevertheless, forecasting wet-snow avalanches is becoming more important in a changing climate. Indeed, by analyzing long-term trends of wet-snow avalanches in the Swiss Alps, Pielmeier et al. (2013) found an increasing number of wet-snow avalanches as well as a temporal shift of wet-snow avalanche cycles towards mid-winter.

* *Corresponding author address:*
Nora Helbig, WSL Institute for Snow and Avalanche Research SLF, Davos, Switzerland;
tel: +41-81-4170-277;
email: norahelbig@gmail.com

In the research outlined in this paper, we therefore focus on the applicability of simple meteorological and terrain parameters for forecasting regional wet-snow avalanche patterns by using avalanche probability maps based on meteorological and terrain parameters. While our approach may not be useable to determine the onset of wet-snow avalanche cycles, since this requires information on the amount of liquid water in the snowpack (Mitterer et al. (2013a)), our goal is mainly to provide a decision making tool to assist avalanche forecasters to better utilize meteorological forecast data in a systematic and objective manner. For this we use large-scale meteorological forecast data of the COSMO model (MeteoSwiss), a parameterization for incident shortwave (SW) radiation accounting for subgrid topographic impacts such as shading, limited sky view and terrain reflections, subgrid mean slope angles, daily avalanche observations and high-quality avalanche observations from a field site above Davos, Switzerland.

2. METHODS AND DATA

2.1 Spatial meteorological and topographical data

Predicting regional wet-snow avalanche patterns requires spatially distributed meteorological data at scales relevant for operational avalanche forecasting. Hourly air temperature (Ta) and incoming SW radiation forecast data of the COSMO-7 model (~7 km horizontal resolution; MeteoSwiss) were therefore downscaled to a 2.5 km grid. Downscaling was performed by bilinear interpolation and temperature adjustments according to elevation using a constant lapse rate of 0.65K/100 m.
Since forecasted incoming SW radiation on a 7 km grid does not account for local topographic influences, we correct the forecasted incident SW radiation for subgrid terrain influences such as shading, terrain reflections and limited sky view. For this, we first extracted terrain parameters such as mean slope angles and the standard deviation of the digital elevation model (DEM) of Switzerland in 25 m horizontal resolution to compute mean sky view factors for the large-scale grid cell sizes of 2.5 km (Helbig and Löwe (2014)). We split the SW radiation value into direct beam and diffuse sky radiation components as described in Helbig et al. (2010). To account for terrain reflections surface albedos on subgrid terrain surfaces are required, which are not necessarily entirely covered by snow. About 300 flat field snow depth values from manual observations and automatic stations were therefore mapped on a DEM of 1 km grid cell size. Detrended snow depth values were then interpolated using a distance-weighting approach based on a Gaussian filter (Jörg-Hess et al. (2014)) and finally spatially averaged to obtain mean snow depth values on a 2.5 km grid. From grid cell mean snow depths, fractional snow-covered area was derived (Helbig et al. (2014)). Fractional snow-covered area was employed to derive mean surface albedo using a mean soil albedo of 0.2 and a mean snow albedo of 0.8 to estimate the amount of reflected SW radiation at subgrid level. Finally, we employed the subgrid parameterization for SW radiation on the splitted SW radiation (Helbig and Löwe (2012); Löwe and Helbig (2012)) using the averaged subgrid terrain parameters and subgrid albedos.

2.2 Avalanche data

Starting in the winter of 2008-2009, we used time-lapse photography to monitor avalanche activity at the Dorfberg field site above Davos, Switzerland (for more details, see van Herwijnen et al., 2013). Over the last six years, we observed 160 avalanches on time-lapse images. The Dorfberg site is also equipped with an automatic weather station, providing continuous meteorological data, including air temperature Ta, incoming SW and longwave (LW) radiation. These data were used to derive probability density functions for air temperature and incoming SW radiation (see Sect. 2.3).

Furthermore, we used spatial avalanche activity data of a widespread wet-snow avalanche cycle in the Swiss Alps, from 1 to 13 March 2013. During this period, observers recorded 937 wet-snow avalanches (Fig. 1). The avalanche cycle includes both, cloudless and clouded sky days. In Switzerland, each observed avalanche is allocated to one of 123 small geographical regions. Since the exact coordinates of an avalanche is unknown, we associated each observation to all 2.5 km grid cells within the small geographical region falling in the same elevation range as the observed release elevation of the avalanche.

2.3 Avalanche probability maps

We used the highly resolved avalanche observations based on time-lapse photography to extract probability density functions (pdf) for meteorological parameters associated with avalanche release. In this context, each pdf describes the avalanche likelihood for a given parameter value. For example, given a certain air temperature Ta, the pdf will give us an avalanche likelihood between 0 (impossibility) and 1 (certainty) defined as the number

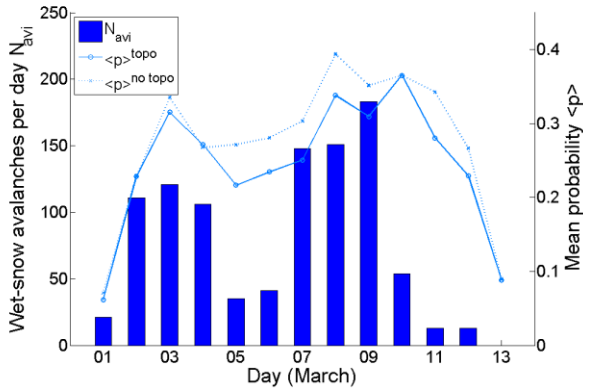

Figure 1. Total number of observed wet-snow avalanches per day in Switzerland. Lines show computed mean probabilities <p> for avalanche grid cells with or without accounting for subgrid topography in SW radiation (<p>^{topo} or <p>$^{no\ topo}$).

of avalanches associated with Ta divided by the total number of occurences of Ta. We derived pdf's (called 'reference' in the following) for two meteorological parameters namely, daily mean Ta and daily mean incoming SW radiation (Fig. 2). Based on a sensitivity study, we determined that using daily means performed best, even though three-day sums were applied in other studies (Mitterer et al. (2013b)). Note that including pdf's for LW radiation did not improve the performance and was therefore neglected.

For each day, we then derived probability maps by comparing a variable's reference pdf to the forecasted corresponding variable, i.e. daily mean Ta and daily mean of parameterized subgrid SW radiation. A combined avalanche probability map was obtained by multiplying the individual probabilities. In a final step, we also included a density distribution for mean slope angles associated with all visual avalanche observations prior to the current day. This was done to account for typical terrain characteristics of the avalanche cycle.

To evaluate the avalanche probability maps, we compared them with daily avalanche observations in Switzerland. To quantify the performance we calculated the probability of detection (POD) and non-detection (PON) as described in Mitterer et al. (2013b). Since avalanche observers do not cover all remote regions and cannot make observations with bad visibility, we did not use a false alarm ratio or the true skill score. Finally, we also compared our probability maps to forecasted avalanche danger maps released by the SLF.

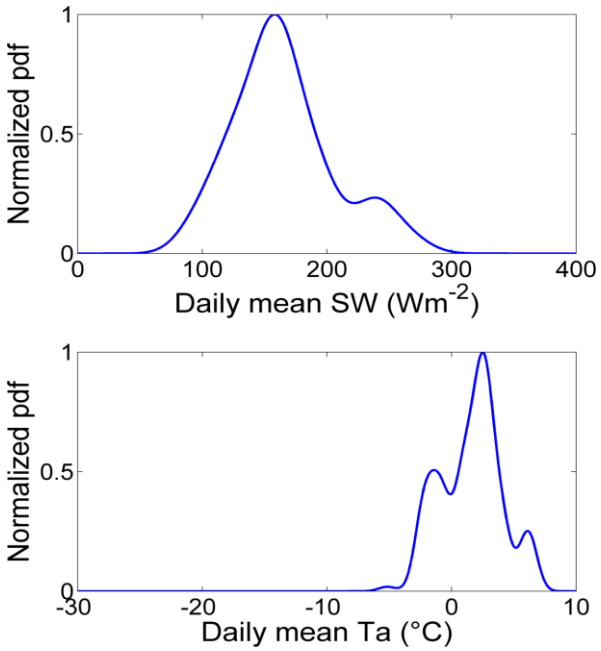

Figure 2. Normalized probability density distribution (pdf) of daily mean air temperature (Ta) and daily mean incident SW radiation (SW) are shown for wet-snow avalanches of the Dorfberg data set.

3. RESULTS AND DISCUSSION

The wet-snow avalanche cycle during the spring of 2013 was characterized by two periods of increased avalanche activity, around 3 and 8 March (Fig. 1). Our computed avalanche probability captured the trend of the total numbers of avalanches per day reasonably well since days with high number of avalanches were generally associated with higher avalanche probability. Overall, the mean avalanche probability improved when accounting for subgrid topography (compare solid and dashed lines in Fig. 1). When not accounting for subgrid topographic influences, daily means of SW radiation were up to 40 Wm^{-2} higher in March over Switzerland. While it is clear that this amount can alter the surface energy balance, subgrid topographic influences are often not accounted for in surface radiation balance computations at larger scales.

Spatial probability maps converted to zeros (probability value=0) and ones (probability>0) reveal distinct terrain patterns over the Swiss Alps. For instance, as seen in Fig. 3 for a cloudy day, avalanche probabilities were zero in valleys. Overall, for the entire wet-snow avalanche cycle, the performance was good in terms of POD's (mean of 0.98) but rather poor in terms of PON's (mean of 0.2). However, the PON values are not reliable since a lack of avalanche observations does not

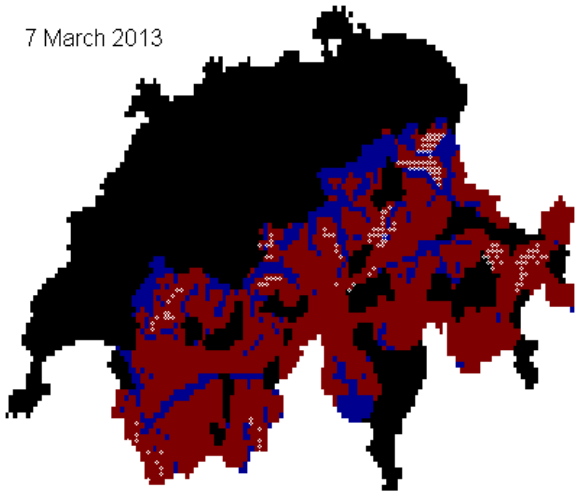

Figure 3. An avalanche probability map is shown for Switzerland with blue indicating a probability of zero, red of one. Black regions are not observed. White dots show observed avalanches; one dot may represent more than one avalanche.

necessarily mean that there was no avalanche activity.

Clearly, binary probability maps are very conservative and overestimate the overall avalanche danger. Indeed, while observed avalanches (white dots in Figure 3) are well predicted (see for example the little region in the upper northeast corner), overall the predicted avalanche danger is high throughout Switzerland. We could easily use a different threshold to discriminate avalanche from non-avalanche grid cells. For instance, the optimal performance for predicting wet-snow avalanches on the Dorfberg was for a probability threshold of 0.2 and resulted in very good mean POD and PON values for all years of 0.87 and 0.70, respectively. However, avalanche prediction is not black and white and requires more levels. We therefore used a logarithmic scale to divide the avalanche probabilities (ranging from zero to one) in three probability levels: lower than 0.1, between 0.1 and 0.32, larger than 0.32. As seen in Figure 4, avalanche probability maps then coincided well with

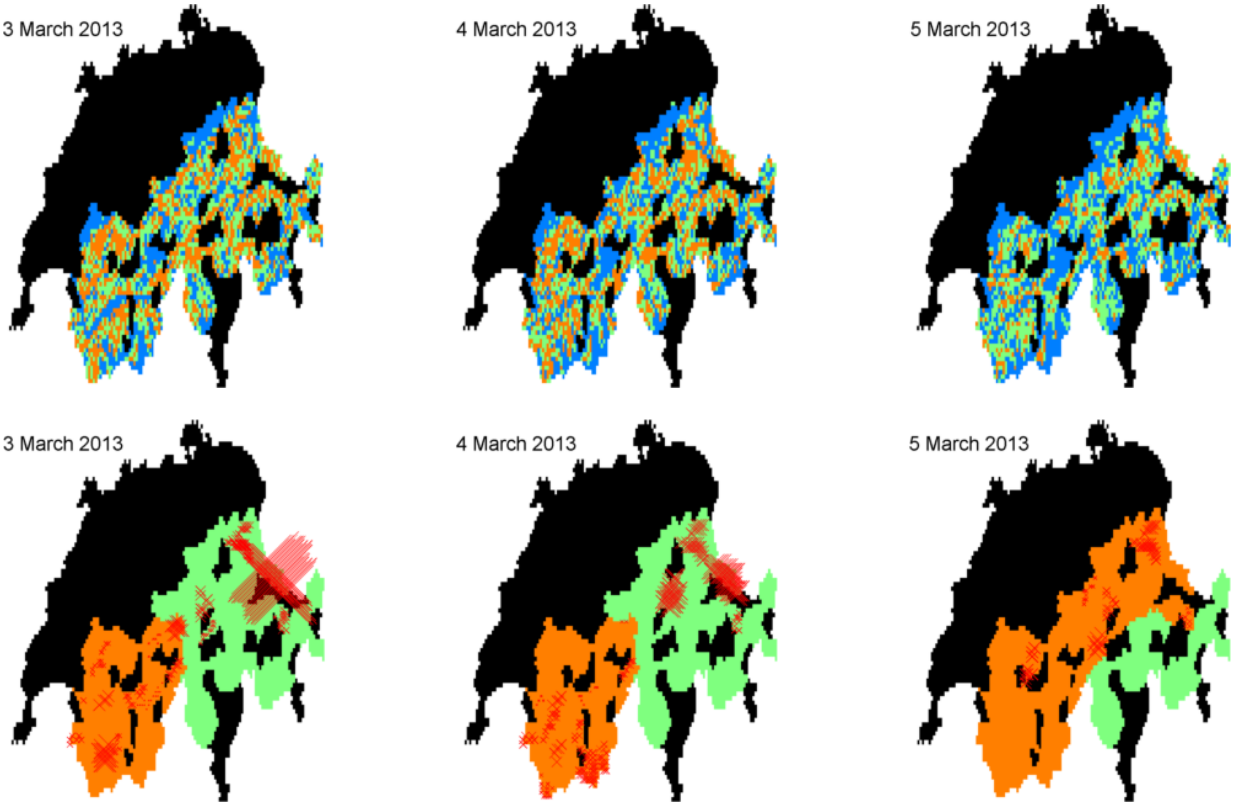

Figure 4. Wet-snow avalanche danger level maps with in blue a score of one, in green of two and in orange of three. Black areas are areas without active avalanche observers or outside avalanche terrain. Red crosses show observed avalanches, the larger the cross the more avalanches. Top: Predicted; Bottom: Predicted wet-snow avalanche danger level.

observed avalanches. Indeed, avalanches were observed all over Switzerland on 3 and 4 March, both cloudless days, and avalanche probability was generally high (level 3; orange in top Fig. 4). On 5 March, a clouded day, avalanche activity was generally lower and more concentrated in Eastern Switzerland. We observed the same spatial pattern in the probability maps, showing also the highest concentration of level 3 probabilities in Eastern Switzerland. Using the probability maps would perhaps have improved the forecasted avalanche danger (bottom Fig. 4), which lagged behind in Eastern Switzerland.

4. CONCLUSIONS AND OUTLOOK

In this study we presented a simple method to create spatial probability maps for wet-snow avalanching. Maps are based on detailed avalanche observations over a six year period derived from time-lapse photography, on meteorological forecast data of air temperature and SW radiation, and on mean slopes of previous avalanches from the current cycle. Our spatial maps show that a simple approach works reasonably well; typical terrain related patterns were clearly captured and even large-scale spatial patterns were realistic. Our method thus may form a step towards automatic avalanche forecasts which would facilitate current avalanche forecasting practices, still largely based on personnel experience. Our approach is not limited to a specific region. For instance, using automatic cameras to obtain detailed avalanche observations, one can easily derive reference density distributions from meteorological data of a nearby automatic station to account for regional climates.

We are well aware that our approach only contributes a small piece to the avalanche forecasting puzzle and that further improvements will require incorporating snow cover information. For instance, accounting for the liquid water content of the snow cover should greatly improve our probability maps. The next step should therefore be to compute all energy balance components spatially while accounting for subgrid topographic influences on the contributing terms, as we now did for SW radiation. However, given the lack of spatially dense accurate avalanche observations, validation of new avalanche maps will remain difficult.

ACKNOWLEDGEMENTS

We would like to thank Christoph Mitterer and Lino Schmid for their assistance in maintaining the time-lapse cameras and the meteorological station at Dorfberg field site during the winter. We also thank the numerous observers who collected the avalanche occurrence data.

REFERENCES

Buser, O., 1983: Avalanche forecast with the method of nearest neighbours: an interactive approach. *Cold Reg. Sci. Technol.*, 8(2), pp. 155-163.

Helbig, N., H. Löwe, B. Mayer and M. Lehning, 2010: Explicit validation of a surface shortwave radiation energy balance model over snow-covered complex terrain. *J. Geophys. Res.*, 115, D18113.

Helbig, N. and H. Löwe, 2012: Shortwave radiation parameterization scheme for sub grid topography. *J. Geophys. Res.*, 117, D03112.

Helbig, N. and H. Löwe, 2014: Parameterization of the spatially averaged sky view factor in complex topography, *J. Geophys. Res. Atmos.*, 119, 4616–4625.

Helbig, N., A. van Herwijnen, J. Magnusson and T. Jonas, 2014: Fractional snow-covered area parameterization over complex topography. *Hydrol. Earth Syst. Sci. Discuss*., 18, pp. 1–37.

Jörg-Hess, S., F. Fundel, T. Jonas and M. Zappa, 2014: Homogenisation of a gridded snow water equivalent climatology for Alpine terrain: methodology and applications. *Cryosphere*, 8, pp. 471-485.

Kattelmann, R., 1985: Wet slab instability, Proceedings of the *International Snow Science Workshop*, Aspen, Colorado, U.S.A., pp. 102-108.

McClung, D.M. and P. Schaerer, 2006: *The Avalanche Handbook.* The Mountaineers, Seattle WA, U.S.A., pp. 342.

Mitterer, C. and J. Schweizer, 2012: Analyzing the atmosphere-snow energy balance for wet-snow avalanche prediction. Proceedings of the *International Snow Science Workshop*, Anchorage, AK, U.S.A., pp. 77-83.

Mitterer, C., F. Techel, C. Fierz and J. Schweizer, 2013a: An operational supporting tool for assessing wet-snow avalanche danger. Proceedings of the *International Snow Science Workshop*, Grenoble, France, pp. 334-338.

Mitterer, C. and J. Schweizer, 2013b: Analyzing the atmosphere-snow energy balance for wet-snow avalanche prediction. *Cryosphere*, 7 pp. 205-216.

Pielmeier, C., F. Techel, C. Marty and T. Stucki, 2013: Wet-snow avalanche activity in the Swiss Alps-trend analysis for mid-winter season. Proceedings of the *International Snow Science Workshop*, Grenoble, France, pp. 1240-1246.

Pozdnoukhov, A., G. Matasci, M. Kanevski and R.S. Purves, 2011: Spatio-temporal avalanche forecasting with Support Vector Machines. *Nat. Hazards Earth Syst. Sci.*, 11(2), pp. 367-382.

Schweizer, J. and P.M.B. Föhn, 1996: Avalanche forecasting - an expert system approach. *J. Glaciol.*, 42(141): 318-332.

Trautman, S., 2008: Investigations into wet-snow. *The Avalanche Review*, 26(4), pp. 16-17.

van Herwijnen, A., N. Berthod, R. Simenhois and C. Mitterer, 2013: Using time-lapse photography in avalanche research. Proceedings of the *International Snow Science Workshop*, Grenoble, France , pp. 950-954.